

Target-responsive aptamer-cross-linked hydrogel sensors for the visual quantitative detection of aflatoxin B₁ using exonuclease I-Triggered target cyclic amplification

Mengyao Zheng^{a,b}, Hongmei Liu^b, Jin Ye^{b,c,d}, Baoxia Ni^b, Yanli Xie^a, Songxue Wang^{a,b,*}

^a College of Food Science and Engineering, Henan University of Technology, Zhengzhou 450001, China

^b Academy of National Food and Strategic Reserves Administration, Beijing 102600, China

^c Key Laboratory of Grain Information Processing and Control (Henan University of Technology), Ministry of Education, Zhengzhou 450001, China

^d Henan Key Laboratory of Grain Photoelectric Detection and Control, (Henan University of Technology), Zhengzhou 450001, China

ARTICLE INFO

Keywords:

Hydrogel
Enzyme cascade
Aptamer
AFB₁
Visual detection

Abbreviations:

aflatoxin B1 (AFB1, PubChem CID: 186907)
Zearalenone (ZEN, PubChem CID: 5281576)
Fumonisin B1 (FB1, PubChem CID: 2733487)
deoxynivalenol (DON, PubChem CID: 40024)
T-2 toxin (T-2, PubChem CID: 5284461)
Aflatoxin G1 (AFG1, PubChem CID: 14421)
Aflatoxin B2 (AFB2, PubChem CID: 2724360)
and Aflatoxin M1 (AFM1, PubChem CID: 15558498)
Ammoniumpersulfate (APS, PubChem CID: 62648)
HRP (PubChem CID: 9865515)
Agarose (PubChem CID: 11966311)
N,N,N',N'-tetramethylethylenediamine (TEMED, PubChem CID: 8037)
3,3',5,5'-tetramethylbenzidine (TMB, PubChem CID: 41206)
H₂O₂ (PubChem CID: 784)

ABSTRACT

For the on-site detection of aflatoxin B₁ (AFB₁), a DNA hydrogel was prepared as a biosensor substrate, while an AFB₁ aptamer was used as the recognition element. An AFB₁-responsive aptamer-cross-linked hydrogel sensor was constructed using an enzyme-linked signal amplification strategy; AFB₁ binds competitively to the aptamer, causing the hydrogel to undergo cleavage and release horseradish peroxidase (HRP). The addition of exonuclease I (ExoI) to the hydrogel causes the release of AFB₁ from the aptamer, promoting additional hydrogel cleavage to release more HRP, ultimately catalysing the reaction between 3,3',5,5'-tetramethylbenzidine and H₂O₂. The hydrogel sensor exhibited an outstanding sensitivity (limit of detection, 4.93 nM; dynamic range, 0–500 nM), and its selectivity towards seven other mycotoxins was confirmed. The feasibility and reliability were verified by measuring the AFB₁ levels in peanut oil (recoveries, 89.59–95.66 %; relative standard deviation, <7%); the obtained results were comparable to those obtained by UPLC-HRMS.

Introduction

The aflatoxins are a class of compounds containing the difuran and coumarin skeletons, and they are produced by fungal strains such as *Aspergillus flavus*, *A. nomius*, and *A. parasiticus* (Xie, Wang, & Zhang, 2019). These compounds have been detected worldwide in agricultural planting, harvesting, storage, transportation, and processing, as well as

in agricultural products, foodstuffs, and animal feeds (Liu, Zhao, Lu, Ye, Wang, Wang, et al., 2020). Among them, aflatoxin B₁ (AFB₁) is the most toxic owing to its strong carcinogenicity, mutagenicity, immunosuppression, and potential to induce liver damage (Fan, Xie, & Ma, 2021). Therefore, the International Agency for Research on Cancer of the World Health Organization has classified AFB₁ as a Class IA dangerous substance and a Class I carcinogen (Xie, Wang, & Zhang, 2019). In addition,

* Corresponding author at: College of Food Science and Engineering, Henan University of Technology, Zhengzhou 450001, China.

E-mail address: wsx@ags.ac.cn (S. Wang).

<https://doi.org/10.1016/j.fochx.2022.100395>

Received 20 May 2022; Received in revised form 29 June 2022; Accepted 12 July 2022

Available online 16 July 2022

2590-1575/© 2022 The Author(s). Published by Elsevier Ltd. This is an open access article under the CC BY-NC-ND license (<http://creativecommons.org/licenses/by-nc-nd/4.0/>).

the U.S. Food and Drug Administration (FDA) has set 20 µg/kg as the permissible limit for AFB₁ in foods (Lerdsri, Thunkhamrak, & Jakmunee, 2021; Xuan, Liu, Ye, Li, Tian, & Wang, 2020). The European Commission has set a 2 µg/kg limit for AFB₁ in some cereals and their derivative products (Commission, 2006). In addition, China's national food safety standard GB 2761–2017 stipulates an AFB₁ limit of 0.5–20 µg/kg in foods (Xuan, Liu, Ye, Li, Tian, & Wang, 2020). Thus, to permit the on-site detection of AFB₁ during food and feed production and processing, especially in underdeveloped areas, it is necessary to develop a portable quantitative AFB₁-detection method with a high sensitivity and specificity.

At present, the market products available for the detection of aflatoxin focus mainly on chromatography-based (Er Demirhan & Demirhan, 2022; Wu, Ye, Xuan, Li, Wang, Wang, et al., 2021; Sarwat, Rauf, Majeed, De Boevre, De Saeger, & Iqbal, 2022; Xuan, Ye, Zhang, Li, Wu, & Wang, 2019) and immunoassay-based (Li, Wang, Sun, Ji, Ye, Lu, et al., 2021; Yan, Zhu, Li, He, Yang, & Liu, 2022; Wang, Zhang, Luo, Qin, Jiang, Qin, et al., 2021) solutions (Li, Wang, Sun, Ji, Ye, Lu, et al., 2021; Wang, Zhang, Luo, Qin, Jiang, Qin, et al., 2021; Yan, Zhu, Li, He, Yang, & Liu, 2022). Although chromatography is highly sensitive and exhibits a good reproducibility, its detection cost is high, it requires large-scale instruments and professional operators, and the sample pretreatment process is relatively complicated (Lerdsri, Thunkhamrak, & Jakmunee, 2021; Xiang, Ye, Shang, Li, Zhou, Shao, et al., 2021). Therefore, this approach is unsuitable for on-site testing. In addition, although the immunoassay-based approach offers some advantages over chromatography (Lerdsri, Thunkhamrak, & Jakmunee, 2021; Xiang, et al., 2021), antibodies are required as recognition elements, which presents new challenges. For example, antibody-based approaches are expensive, a poor thermal stability, and difficulty in terms of the transportation and storage, thereby hindering the development and application of immunological technologies (Ni, Zhuo, Pan, Yu, Li, Liu, et al., 2020). To address these issues, in the early 1990s, Ellington and Szostak obtained a nucleic acid sequence after multiple rounds of Systematic Evolution of Ligands by Exponential Enrichment (SELEX), which they named an "aptamer (Ellington & Szostak, 1990)." Aptamers are of interest because can be easily prepared and modified, and they are also known to exhibit a strong thermal stability, low immunogenicity properties, almost no batch-to-batch variation, and facile storage and transportation; as such, they are expected to replace antibodies for various applications (Ni, et al., 2020). In recent years, there have been many reports on the application of aptamers in the detection of mycotoxins, such as in target-responsive DNA smart hydrogel sensors (Liu, Huang, Ma, Jia, Gao, Li, et al., 2015; Sun, Li, Chen, Wu, & Liang, 2020), electrochemical sensors (Jahangiri-Dehaghani, Zare, Shekari, & Benvidi, 2022; Zhong, Li, Li, JiYe, Mo, Chen, et al., 2022; Chen, Li, Meng, Liu, Liu, Dong, et al., 2022; Zhong, Li, Li, JiYe, Mo, Chen, et al., 2022) (Jahangiri-Dehaghani, Zare, Shekari, & Benvidi, 2022), fluorescence colorimetric sensors (Setlem, Mondal, & Ramlal, 2022; Zhang, Mao, Hu, Wei, Huang, Fan, et al., 2022; He, Sun, Pu, & Huang, 2020; Qi, Lv, Wei, Lee, Niu, Cui, et al., 2022) etc. Among them, target-responsive DNA smart hydrogel sensors have attracted extensive attention owing to their flexibility, stability, cost-effectiveness, portability, and ease of storage, and they are considered to have great prospects for application in the field of on-site detection.

It has been reported that aptamers such as glucose (Ma, Mao, An, Tian, Zhang, Yan, et al., 2018), Pb²⁺ (Huang, Ma, Chen, Wu, Fang, Zhu, et al., 2014), and ochratoxin (Liu, et al., 2015) can be used as cross-linking agents for hydrogels to embed gold nanoparticles (AuNPs). When a target is detected, the hydrogel is cleaved and the AuNPs are released, thereby turning the supernatant a red colour. Although this method can be used to determine the concentration of a target substance, its sensitivity is generally poor, and it is difficult to meet the threshold of the limit of detection for most applications. To overcome these shortcomings, Huang (Huang, et al., 2014) and Liu (Liu, et al., 2015) replaced AuNPs with platinum nanoparticles (PtNPs), and found that the released PtNPs catalysed the decomposition of H₂O₂ to O₂,

which then causes the pigment to move on a microfluidic chip, and results in concentration of the target for facile detection. In addition, Tang (Tang, Huang, Lin, Qiu, Guo, Luo, et al., 2020) used the air pressure generated by PtNPs to catalyse the decomposition of H₂O₂ into O₂, which promoted the discharge of water. The concentration of the target was then determined by weighing the obtained water with an analytical balance. Whether performed with a microfluidic platform or an analytical balance, this method relies on the device being air-tight, and the instrument exhibiting a high precision. Furthermore, the design of the microfluidic platform requires the participation of different professionals, which largely limits its popularisation and application.

Thus, we herein report the construction of an AFB₁-responsive DNA smart hydrogel sensor using a high-affinity and high-specificity AFB₁ aptamer as the cross-linking agent and recognition element; this construction is combined with an enzyme cascade signal amplification strategy. During hydrogel formation, horseradish peroxidase (HRP) becomes encapsulated inside the hydrogel, and it remains encapsulated until the hydrogel undergoes cleavage. Upon the addition of AFB₁, aptamer binding takes place, resulting in cleavage of the hydrogel and the release of HRP. Subsequently, the addition of exonuclease I (ExoI) specifically recognises and cleaves the AFB₁-aptamer complex, thereby releasing AFB₁. AFB₁ again competes with the aptamer for binding, resulting in further hydrogel cleavage and the release of additional HRP, which catalyses the generation of oxygen free radicals from H₂O₂ outside the hydrogel system. These free radicals promote the colour development of 3,3',5,5'-tetramethylbenzidine (TMB), thereby achieving the highly-sensitive and highly-specific visual and quantitative detection of AFB₁. Finally, this method is applied for the detection of AFB₁ in peanut oil samples, and its accuracy and consistency are compared with those obtained by UPLC-HRMS to determine its feasibility for use in the detection of AFB₁ in underdeveloped areas.

Materials and methods

Chemicals and materials

ExoI and 10 × ExoI reaction buffer (pH 7.5) were purchased from Thermo Fisher Scientific (Shanghai, China) and were stored at −20 °C. Ammonium persulfate (APS, PubChem CID: 62648) was purchased from Kulaibo Technology Co., Ltd (Beijing, China), N,N,N',N'-tetramethylethylenediamine (TEMED, 100 %, PubChem CID: 8037) was purchased from Merck Investment (China) Co., Ltd. Standard solutions such as AFB₁ (PubChem CID: 186907), Zearalenone (ZEN, PubChem CID: 5281576), Fumonisin B₁ (FB₁, PubChem CID: 2733487), deoxynivalenol (DON, PubChem CID: 40024), T-2 toxin (T-2, PubChem CID: 5284461), Aflatoxin G₁ (AFG₁, PubChem CID: 14421), Aflatoxin B₂ (AFB₂, PubChem CID: 2724360), and Aflatoxin M₁ (AFM₁, PubChem CID: 15558498) were purchased from Biopure (Tulln, Austria) and was stored at −20 °C. Working solutions were prepared by dilution with HPLC grade methanol, and then stored in vials at 4 °C and were renewed weekly. HRP (PubChem CID: 9865515), TMB (PubChem CID: 41206) and H₂O₂ (PubChem CID: 784) were purchased from Solarbio Science & Technology Co., Ltd. (Beijing, China), while Acr-Bis(29:1) and acrylamide were purchased from Beijing Coolibo Technology Co., Ltd. and was stored at 4 °C prior to use. Furthermore, 10 × Tris-borate-EDTA (TBE) buffer was purchased from Sangon Biological Engineering Technology & Services Co., Ltd. (Shanghai, China), phosphate-buffered saline (PBS) solution was purchased from HyClone Laboratories Inc (USA), and agarose (PubChem CID: 11966311) and the TAE (Tris base, acetic acid, and EDTA) buffer solution were purchased from Soleibao Technology Co., Ltd. (Beijing, China). NHS activated magnetic beads was purchased from Beaver (Suzhou, China).

All oligonucleotides were synthesised by Sangon Biotech Co., Ltd. (Shanghai, China). Their sequences are shown below:

Strand A: 5'-Acrydite-TTTTGTGGGCCTAGCGA-3'.

Strand B: 5'-Acrydite-TTTACACGTGCCAAC-3'.

Aptamer-linker: 5'-GTTGGGCACGTGTGTCTCTCTGTGTCTCGTGC CCTT CGCTAGGCCACA-3'; the sequence for the AFB₁ aptamer has been reported in previous studies (Hosseini, Khabbaz, Dadmehr, Ganjali, & Mohamadnejad, 2015; Wang, Chen, Wu, Weng, Liu, Lu, et al., 2016; Wu, Zhu, Xue, Mei, Yao, Wang, et al., 2014).

Preparation of polymers PS-A and PS-B

Referring to the method of Si (Si, Li, Wang, Zheng, Yang, & Li, 2019) 25 % acrylamide (4 μ L) was mixed with PBS buffer solution (12 μ L), followed by 4 mM of an acrylamide-labelled Strand A or Strand B solution (8 μ L), which was mixed and degassed in a vacuum dryer for 10 min. Subsequently, a 5 % solution of APS (1 μ L, the solvent is ultrapure water) and a 5 % solution of TEMED (1 μ L, the solvent is ultrapure water) were added and mixed evenly. After degassing in a vacuum dryer for 18 min, the polymers were purified using a 100 kDa ultrafiltration centrifuge, redissolved in PBS buffer, and stored at 4 °C for later use. The PS-A and PS-B polymers were quantified using NanoDrop spectrophotometry and characterised by means of 2 % agarose gel electrophoresis.

Preparation of the AFB₁ responsive aptamer-cross-linked hydrogels

Polymers PS-A and PS-B (2 μ L each, 200 μ M solutions) were mixed, placed in a metal bath, and incubated at 55 °C for 5 min, and then at 27 °C for 5 min; this double incubation process was repeated twice. Subsequently, HRP (1 μ L, 8 mg/L) and the AFB₁ aptamer (2 μ L, 190 μ M) were added and mixed, and the resulting mixture was placed in a metal bath for incubation at 55 °C for 5 min, and then at 27 °C for 5 min. This incubation process was repeated 6 times to yield a 3D cross-linked DNA hydrogel embedded with HRP, as characterised by 20 % PAGE gel electrophoresis.

AFB₁ detection based on amplification of the ExoI enzyme signal

Under the optimal conditions, referring to the method described in Tang's study (Tang, et al., 2020), 20 U exonuclease ExoI was introduced into the system to further amplify the signal and improve the sensitivity of the method. More specifically, for detection of the target AFB₁, an aliquot (50 μ L) of the AFB₁ sample solution containing 20 U ExoI (methanol content < 10 %) was added to a centrifuge tube containing the DNA hydrogel and reacted at 150 rpm and 25 °C for 1.5 h (Ma, Mao, Huang, He, Yan, Tian, et al., 2016). Subsequently, an aliquot (25 μ L) of the supernatant was employed for the colour-generating reaction with TMB (100 μ L). After 20 min, a 1 M HCl solution (100 μ L) was used to quench the reaction. The absorbance of the supernatant was measured at 650 nm before quenching with hydrochloric acid, and at 453 nm after quenching.

Evaluation of the detection performance

Under the optimal conditions, AFB₁ was added to the system at concentrations of 0, 100, 200, 300, 400, and 500 nM to investigate the visual detection performance of the hydrogel sensor. The specificity of the method was verified by the analysis of a 100 nM AFB₁ solution and 1 μ M solutions of AFB₁ structural analogues, such as zearalenone (ZEN), fumonisin B₁ (FB₁), deoxynivalenol (DON), T-2 toxin (T-2), aflatoxin G₁ (AFG₁), aflatoxin B₂ (AFB₂), and aflatoxin M₁ (AFM₁).

Procedure for real sample processing

According to the method described by Xuan (Xuan, Ye, Zhang, Li, Wu, & Wang, 2019), AFB₁ immune affinity magnetic beads were used on an automatic purification apparatus to extract and purify AFB₁ from peanut oil. More specifically, the peanut oil sample (0.25 mL, ~0.221 g), a 0.5 % PBST solution (0.45 mL), and the immune affinity magnetic beads (150 μ L) were mixed in the reaction well. A 0.5 % PBST solution

(2 mL) was evenly divided into two cleaning wells, and PBS (1 mL) was placed in another cleaning well. The extraction principle involved the AFB₁ present in peanut oil being captured by the AFB₁ antibody fixed on the magnetic beads. After cleaning three times, the AFB₁ fixed on the magnetic beads was eluted with methanol, and the volume was fixed to 1.2 mL. After filtration through a 0.2- μ m filtration membrane, an aliquot was taken for quantitative analysis by UPLC-HRMS, while the other aliquot was subjected to the developed method for AFB₁ detection.

Results and discussion

Preparation of the hydrogel biosensor and its AFB₁ detection mechanism

To prepare the hydrogel biosensors, two acrydite-modified nucleic acids were initially prepared, namely Strand A and Strand B, which can be paired with the complementary bases at both ends of the cross-linking agent (i.e., the AFB₁ aptamer), which is located within the hydrogel. Under the catalysis of APS and TEMED, Strands A and B were copolymerised in the presence of the acrylamide monomer to form polymers PS-A and PS-B, respectively. The aptamer was then linked to PS-A and PS-B to form DNA hydrogels. During hydrogel formation, HRP was added, resulting in its embedding inside the hydrogel. When the target AFB₁ is present, it binds competitively to the nucleic acid aptamer, resulting in the cleavage and collapse of the hydrogel. The addition of ExoI then leads to the specific recognition and cleavage of the AFB₁-aptamer complex, thereby releasing AFB₁, which then again competes with the aptamer for binding, resulting in further hydrogel cleavage and the release of a large amount of HRP. The released HRP then catalyses the generation of oxygen free radicals from H₂O₂ outside the hydrogel, and these free radicals then promote the colour change of TMB. More specifically, a blue solution was obtained in the presence of AFB₁, yielding an absorbance peak at 650 nm. After termination of the reaction using hydrochloric acid, the solution turned yellow giving an absorbance peak at 453 nm. The intensities of these peaks (i.e., the peak absorbances) were found to vary depending on the content of AFB₁ present, thereby confirming the visual and quantitative detection of AFB₁. The principle of operation of the aptamer-cross-linked hydrogel sensors is illustrated in Fig. 1.

Characterisation of PS-A and PS-B and the mechanism of hydrogel formation

The characterisation of polymers PS-A and PS-B was carried out by means of 2 % agarose gel electrophoresis, and the results are shown in Fig. 2A. Compared with Strand A (lane 1) and Strand B (lane 3), the migration rates of polymers PS-A (lane 2) and PS-B (lane 4) were low, thereby indicating that the molecular weights of PS-A and PS-B were significantly higher than those of their predecessors, namely Strands A and B, respectively. This is consistent with the results of the study by Ma (Ma, et al., 2018), indicating that polymers PS-A and PS-B were successfully prepared. In addition, the observation of lanes 5, 6, and 7 also showed that 2 % agarose gel electrophoresis was not suitable for characterising the mechanism of hydrogel formation.

Therefore, 20 % non-denaturing polyacrylamide gel electrophoresis (PAGE) was used to characterise the mechanism of formation of the AFB₁-responsive aptamer-cross-linked hydrogel (Ma, et al., 2016). As shown in Fig. 2B, comparisons between Strand A (lane 1) and PS-A (lane 3), and Strand B (lane 2) and PS-B (lane 4) showed that nucleic acids were retained in the injection port after polymer formation. Furthermore, the migration rate of Strand B (PS-B) was higher than that of Strand A (PS-A), which also indicates that the molecular weight of Strand B (PS-B) is lower than that of Strand A (PS-A). By comparing PS-A (lane 3), PS-B (lane 4), the aptamer (lane 5), PS-A + aptamer (lane 6), PS-B + aptamer (lane 8), and PS-A + aptamer + PS-B (lane 11), the positions of the binding bands of the various component could be easily identified, as indicated in the figure. Theoretically, according to the

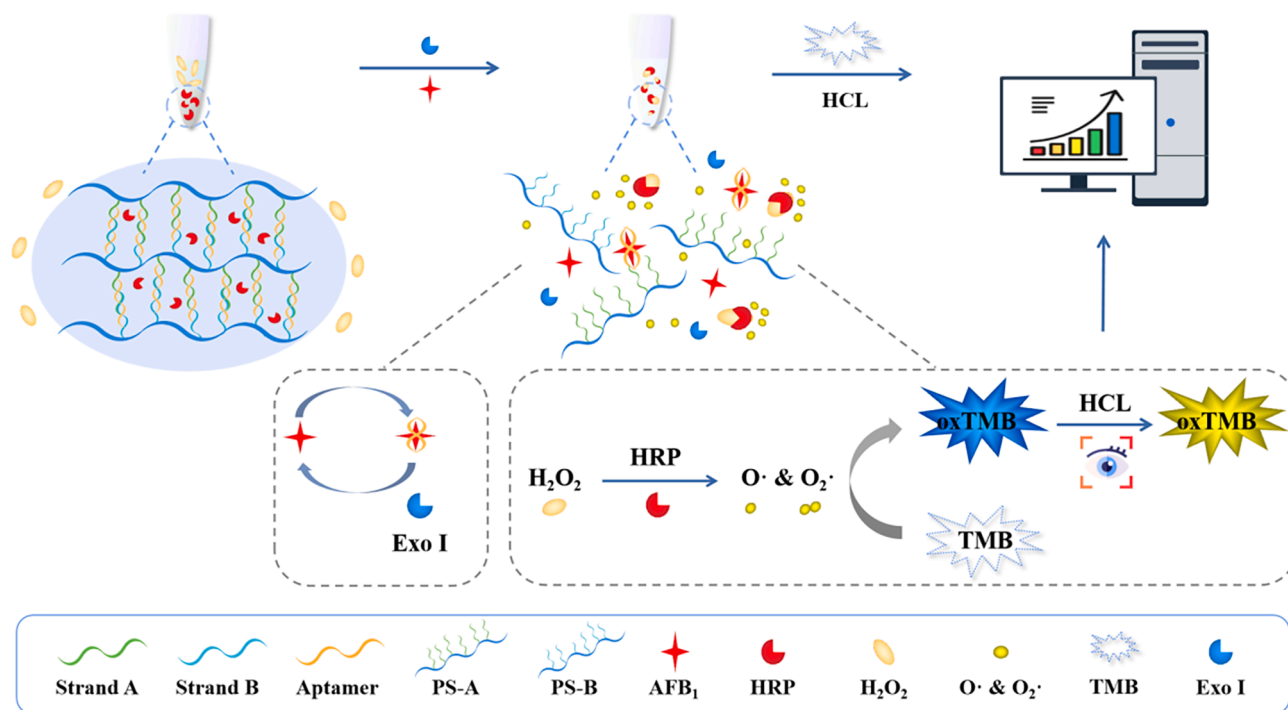


Fig. 1. Detection principle of AFB₁-responsive aptamer-functionalized DNA intelligent hydrogel.

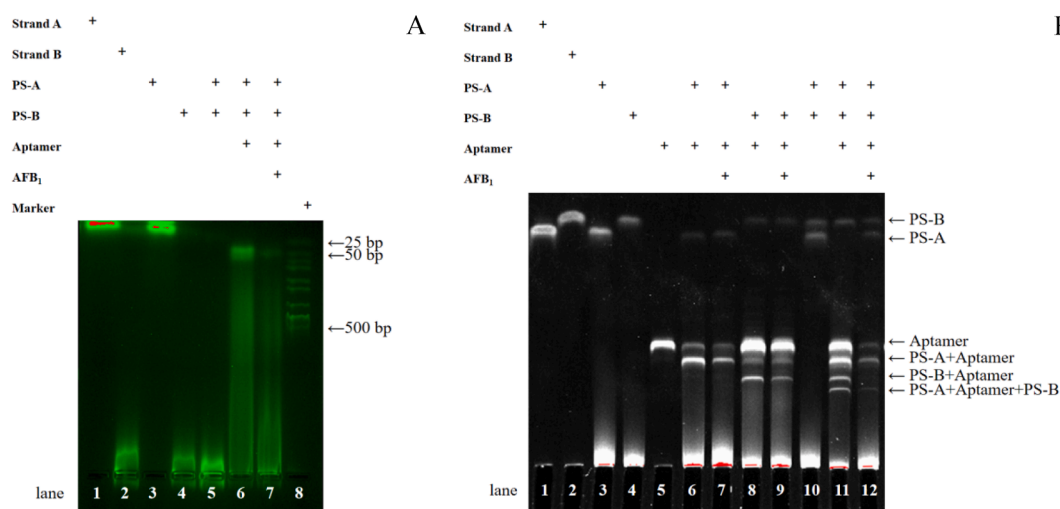


Fig. 2. A) the formation of polymers PS-A and PS-B; and B) intelligent hydrogel formation based on AFB₁-aptamer DNA.

molecular weight, the mobility of the PS-B + aptamer band should be higher than that of the PS-A + aptamer band, but in fact, the opposite result was obtained. This suggests that the combination of PS-B with the aptamer leads to a change in the aptamer conformation, which then alters the mobility. In addition, the brightness of the aptamer-containing bands decreased after the addition of AFB₁, while the brightness of the aptamer and PS-B + aptamer bands decreased significantly. It was therefore inferred that the of the PS-B/aptamer hybridisation region and the AFB₁ binding site intersect, which is consistent with the results of the study by Ma (Ma, et al., 2016). Moreover, based on the observation of lane 10 (i.e., PS-A + PS-B), in the absence of the aptamer, no interactions took place between PS-A and PS-B.

Optimisation of the concentration of each component

The strength of the hydrogel depends on the polymer and aptamer

concentrations, wherein a higher concentration leads to a stronger hydrogel. In contrast, low concentrations of the polymer and the aptamer render the hydrogel prone to cracking, which prohibits the complete encapsulation of HRP, thereby rendering it difficult to detect AFB₁. Therefore, to form a hydrogel with a suitable strength and sensitivity, two ratios of PS-A:PS-B:aptamer were initially determined to be suitable, namely 1:1:0.5 and 1:1:1. More specifically, during optimisation, these ratios were found to enable a sufficient amount of HRP embedding into the hydrogel to explore the optimal concentrations of polymers PS-A and PS-B. As shown in Fig. 3A, with a polymer concentration of 200 μ M and a PS-A:PS-B:aptamer ratio of 1:1:1, macroscopic hydrogels were formed. The photographic images shown in this figure indicate that the zero boundary of each macroscopic hydrogel was present at a polymer concentration of 200 μ M and an aptamer concentration between \sim 100 and 200 μ M.

Furthermore, if the concentration of HRP is too high, complete

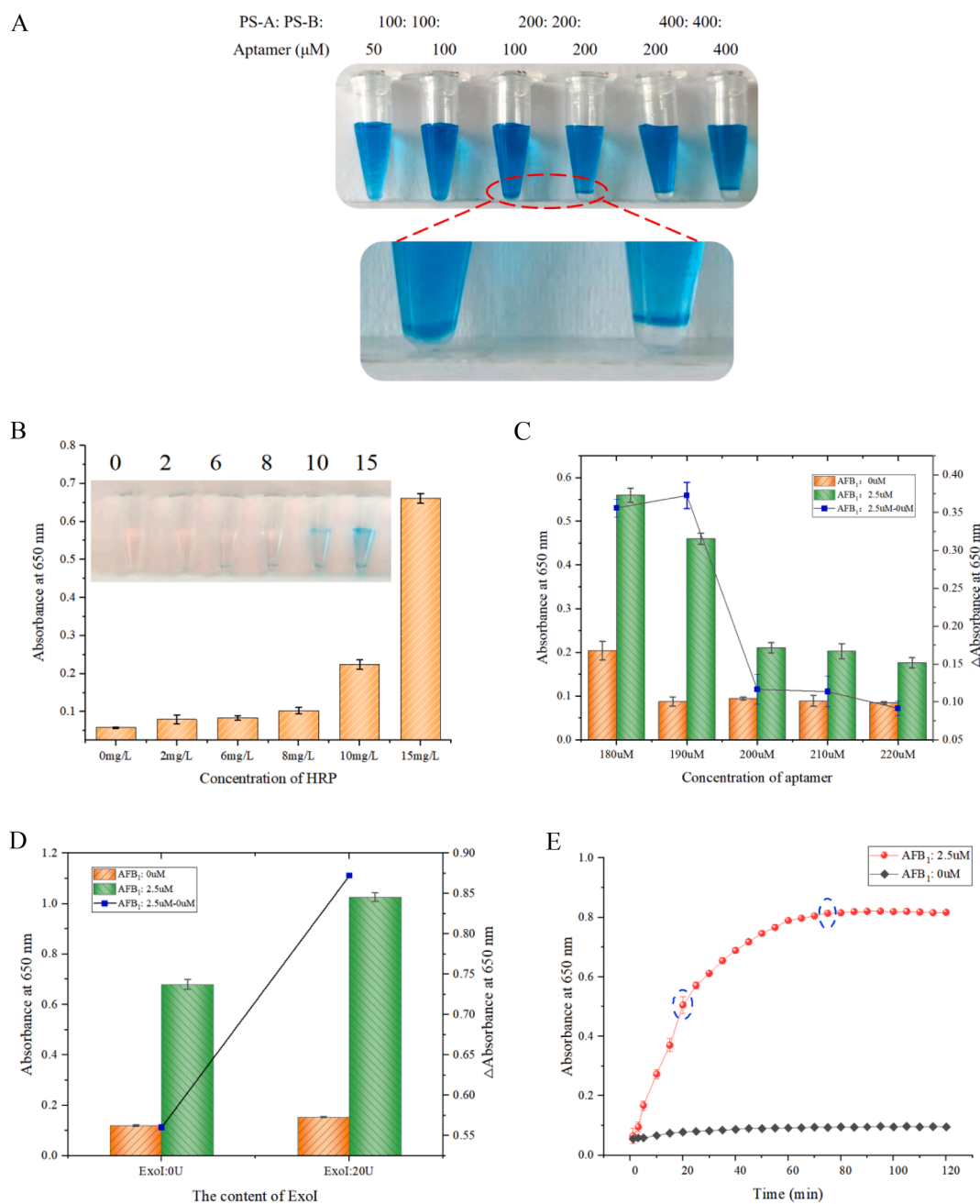


Fig. 3. A) Optimization of polymer PS-A and PS-B concentration; B) Optimization of horseradish peroxidase concentration; C) Optimization of aptamer concentration; D) ExoI signal amplification mechanism characterization; E) Optimization of color rendering time.

embedding was not achieved, resulting in a large background signal that interferes with the detection results. Conversely, if the concentration of HRP is too low, the cleavage response signal is also low, resulting in a poor sensitivity of the detection method. Thus, to optimise the concentration of HRP, the polymers and the aptamer (200 μM each) were combined in a 1:1:1 ratio, and the HRP concentration was varied across six samples. As shown in Fig. 3B, at HRP concentrations of 2, 6, and 8 mg/L, the background signal value is relatively small. However, upon increasing the HRP concentration to 10 mg/L, the background signal is more than double that obtained at 8 mg/L. Furthermore, at a concentration of 15 mg/L, a higher background signal was observed once again, and so an HRP concentration of 8 mg/L was considered to be optimal.

Optimisation of the aptamer concentration was then performed in the concentration range of 180–220 μM , as shown in Fig. 3C. It was found that not only the hydrogel cleavage signal formed in the presence

of 180 μM aptamer (i.e., the signal corresponding to 2.5 μM AFB₁), but also the associated background signal (i.e., the signal value corresponding to 0 μM AFB₁) were the largest signals. The background signals for the remaining four concentrations (i.e., 190, 200, 210, and 220 μM) were relatively comparable (OD < 0.1), although a slightly superior result was obtained for an aptamer concentration of 190 μM , and so this was selected as the optimal aptamer concentration.

Signal amplification strategy

ExoI was introduced into the experiment to obtain superior sensitivity over a relatively short period of time. More specifically, according to a study by Tang (Tang, et al., 2020), ExoI can assist AFB₁ in splitting the hydrogel and releasing additional HRP to further catalyse the colour development of TMB. Indeed, as shown in Fig. 3D, the introduction of

ExoI increased the difference between the cleavage signal and the background signal by 1.56 times, which demonstrated that ExoI can assist AFB₁ in cleaving the hydrogel. The released HRP then catalyses the reaction between H₂O₂ and TMB. Prior to quenching the reaction with hydrochloric acid, the reaction signal initially increased sharply prior to stabilising after 75 min. As shown in Fig. 3E, the rate of increase in the signal value is most pronounced during the initial 20 min. Thus, to shorten the detection time as much as possible, 20 min was selected as the optimal colour development time. As a result of this process, the detection range of the sensor can be increased or decreased by adjusting the reaction time within a certain range.

Visual quantitative detection of AFB₁

Under the optimised conditions, a range of AFB₁ concentrations were investigated to demonstrate the quantitative detection of this toxin. As shown in Fig. 4A and 4B, upon increasing the concentration of AFB₁, the solution colour become more intense, and the corresponding absorbance value gradually increased, showing a positive linear relationship that can be fitted with the equation: $y = 0.0012x + 0.1453$ ($R^2 = 0.9943$). The limit of detection for AFB₁ based on this method was therefore estimated to be 4.93 nM (signal-to-noise ratio = 3).

A comparison of our AFB₁-responsive DNA smart hydrogel with some previously reported systems is presented in Table 1. Although the hydrogel constructions were essentially comparable between these systems, the embedding materials were different. In addition to the

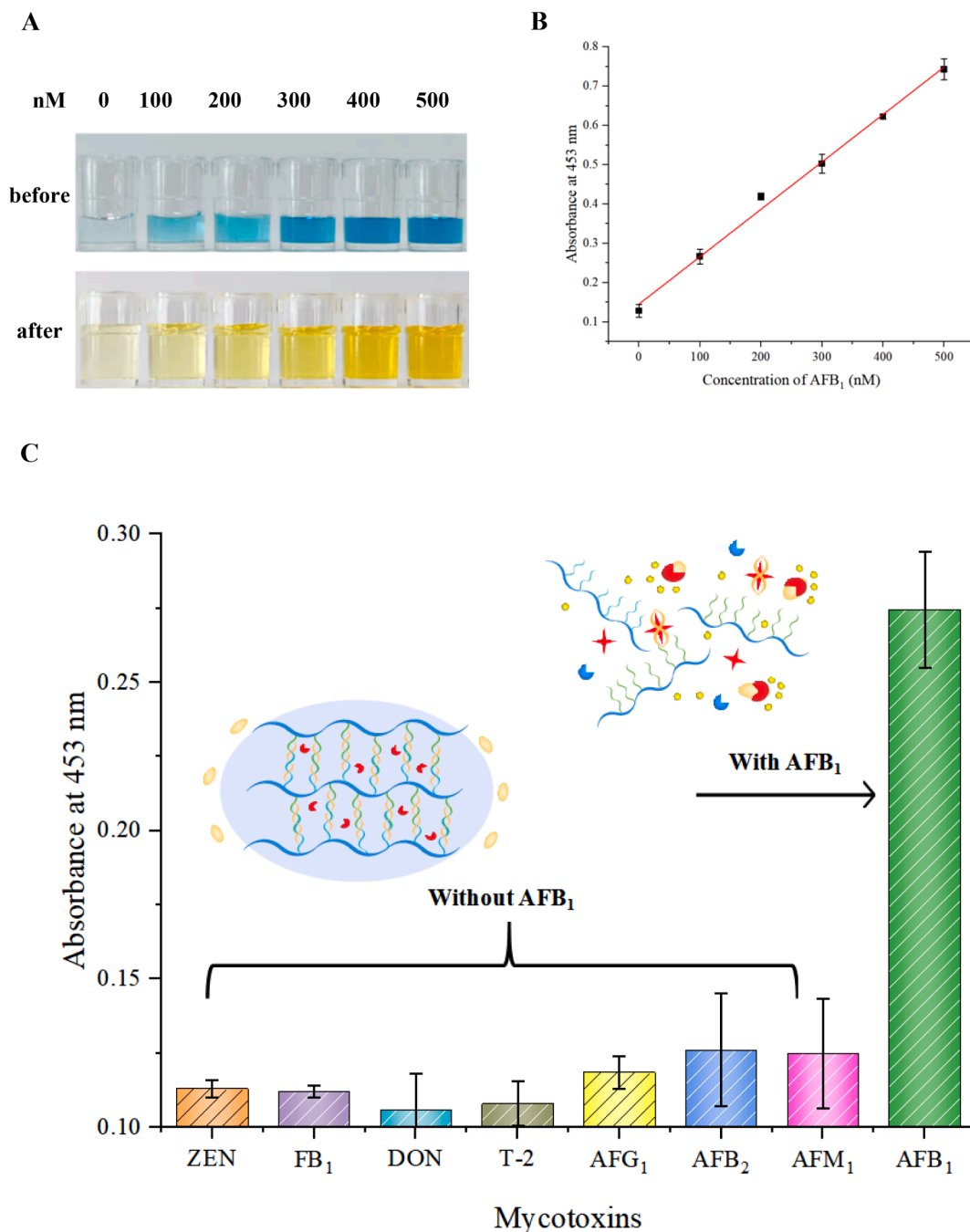


Fig. 4. A) Colorimetric results of hydrogel sensor detection of different concentrations of AFB₁ before and after hydrochloric acid termination; B) Standard fit for the detection of different concentrations of AFB₁ based on hydrogel sensor; C) Specificity of AFB₁ detected by aptamer DNA smart hydrogel.

Table 1
Compared with other reported AFB₁-responsive DNA smart hydrogel sensor.

Embedded material	Signal amplification	detection method	detection limit	detection range	Recovery	references
PtNPs	micro-fluidic chip	AFB ₁ splits the hydrogel and releases PtNPs. PtNPs catalyze the decomposition of H ₂ O ₂ to generate O ₂ , which promotes the movement of pigments on the microfluidic chip	1.77 nM	0.25–40 μM	–	(Ma, et al., 2016)
AuNPs	–	AFB ₁ splits the hydrogel and releases AuNPs, which change the color of the supernatant from colorless to red.	0.21 μM	0.25–10 μM	–	(Ma, et al., 2016)
PtNPs	Exo I	AFB ₁ splits the hydrogel to release PtNPs. PtNPs catalyze the decomposition of H ₂ O ₂ to generate O ₂ , and the air pressure promotes the discharge of water, which is weighed by an analytical balance.	9.4 μg/kg	31.2 μg/kg – 6.2 mg/kg	91.5 % –98.1 %	(Tang, et al., 2020)
urease	–	AFB ₁ splits the hydrogel, releases urease, and urease hydrolyzes urea, which changes the pH of the solution.	0.1 μM	0.2–20 μM	82.26 % –89.43 %	(Zhao, Wang, Guo, Wang, Luo, Qiu, et al., 2018)
HRP	Exo I	Exo I assists AFB ₁ to split the hydrogel, releasing HRP. HRP catalyzes the color reaction between TMB and H ₂ O ₂ , and the concentration of AFB ₁ in solution is obtained according to the change of color and absorbance value.	4.93 nM (8.395 μg/kg)	0–500 nM (0–847.79 μg/kg)	89.59 % –95.66 %	This work

Table 2
Comparison between this experimental method and UPLC-HRMS in actual sample detection results.

Sample	Added (μg/kg)	Standard addition concentration (nM)	Developed sensor				UPLC-HRMS					
			Detected (nM)	Recovery (%)	Average recovery (%)	RSD (%)	Detected (nM)	Recovery (%)	Average recovery (%)	RSD (%)		
peanut oil	0	0	ND	–	–	–	ND	–	–	–		
			5.78	97.97 %	89.59 %	6.61 %	5.37	91.08 %	95.44 %	3.25 %		
			5.04	85.41 %			5.73	97.19 %				
	20	11.7953	5.04	85.41 %			5.78	98.03 %				
			10.96	92.94 %	92.94 %	2.76 %	11.77	99.80 %	99.97 %	0.91 %		
			10.59	89.80 %			11.67	98.95 %				
40	23.5907	11.33	96.08 %			11.93	101.16 %					
		22.44	95.14 %	95.66 %	2.05 %	23.10	97.91 %	98.38 %	0.92 %			
		22.07	93.57 %			23.51	99.64 %					
			23.19	98.28 %					23.02	97.58 %		

nanoparticles mentioned in the introduction, target-responsive hydrogels have also been embedded with encapsulated enzymes (Mao, Li, Yan, Ma, Song, Tian, et al., 2017; Si, Li, Wang, Zheng, Yang, & Li, 2019; Ma, et al., 2016). For example, Tian and his colleagues (Tian, Wei, Jia, Zhang, Li, Zhu, et al., 2016) used an amylase released during hydrogel cleavage to hydrolyse starch to glucose, wherein the glucose was subsequently oxidised to H₂O₂ by the glucose oxidase enzyme. Under catalysis by HRP, the generated H₂O₂ underwent a redox reaction with KI to generate brown I₂. On this basis, Wei and his colleagues (Wei, Tian, Jia, Zhu, Ma, Sun, et al., 2016) replaced KI with diaminobenzidine, a chromogenic substrate of HRP, and realised the detection of cocaine. In addition, Si and his colleagues (Si, Li, Wang, Zheng, Yang, & Li, 2019) simplified the reaction steps to directly measure the concentration of glucose by means of a blood glucose meter. Furthermore, Sun and his colleagues (Sun, Li, Chen, Wu, & Liang, 2020) used the HRP released by the hydrogel cleavage to catalyse the redox reaction between H₂O₂ and KI. The generated I₂ was then used to etch gold nanorods (AuNRs), resulting in a wavelength shift, which allowed the content of a T-2 toxin to be estimated with a good sensitivity and accuracy. However, despite these advances, there are few reports on the use of AFB₁-responsive DNA smart hydrogels to encapsulate enzymes. Our method uses a cascade of enzyme reactions, and the introduction of ExoI achieves the desired cycle amplification and promotes the release of additional HRP to further catalyse the colour-generating reaction between TMB and H₂O₂, ultimately realising a dual signal amplification strategy. In addition, our system shows certain advantages in terms of its detection range, as indicated in the table.

Detection selectivity

To investigate the specificity of the developed hydrogel biosensor, we introduced additional toxins in combination with AFB₁, i.e., ZEN, FB₁, DON, T-2, AFG₁, AFB₂, and AFM₁. The concentration of AFB₁ was set at 100 nM, while the concentrations of the other toxins were set at 1 μM. The results of the assay are shown in Fig. 4C, wherein the advantages of the aptamer-based approach can be clearly observed. More specifically, although the concentration of AFB₁ was only 10 % that of each other toxin, its signal was 2–3 times more intense than those of the other toxins, confirming the specificity of the sensor toward our target toxin.

Determination of AFB₁ contents in real samples

Finally, the developed hydrogel biosensor was used to test peanut oil samples containing AFB₁. Thus, AFB₁ concentrations of 10, 20, and 40 μg/kg were added to the peanut oil samples; these concentrations are equivalent to 0.5, 1, and 2 times the 20 μg/kg limit specified by the FDA. Each sample was then pre-treated according to the experimental method described in Section 2.6, and the content of AFB₁ in each peanut oil sample was measured by both UPLC-HRMS and using our hydrogel biosensor. As outlined in Table 2, the average spiked recoveries obtained for the hydrogel biosensor and by UPLC-HRMS were approximately 89.59–95.66 % and 95.44–99.97 %, respectively, with RSD values of < 7 % in both cases. This comparison therefore confirms the accuracy and repeatability of our method, and indicate its potential for use in the detection of AFB₁ in real samples.

Conclusions

We constructed and tested a smart aptamer-based DNA hydrogel biosensor for the quick and accurate on-site detection of aflatoxin B₁ (AFB₁). An AFB₁ aptamer with a high affinity and specificity was used as the cross-linking agent and recognition element of the hydrogel, and the cascade enzyme reaction signal amplification strategy was used to successfully construct the AFB₁ responsive aptamer-cross-linked hydrogel sensor. The linear range of the sensor was ~ 0–500 nM, its limit of detection was 4.93 nM (signal-to-noise ratio = 3), and its accuracy and repeatability were comparable to those of UPLC-HRMS. Overall, our results indicate the potential of this sensor to be used for the highly sensitive on-site detection of AFB₁ in underdeveloped areas.

Funding

This work was supported by the Open Fund Project of the Key Laboratory of Grain Information Processing & Control (Ministry of Education, Henan University of Technology, China) (KFJJ-2020-102); the National Natural Science Foundation of China (31901806 and 81803712); the Young Elite Scientists Sponsorship Program by CAST (2021QNRC001); Beijing Municipal Natural Science Foundation Grant numbers (7192026)

CRedit authorship contribution statement

Mengyao Zheng: Conceptualization, Data curation, Formal analysis, Investigation, Methodology, Project administration. **Hongmei Liu:** Conceptualization, Resources, Methodology, Formal analysis, Validation. **Jin Ye:** Methodology, Formal analysis, Project administration, Resources. **Baoxia Ni:** Methodology, Project administration, Writing – review & editing. **Yanli Xie:** Supervision, Validation, Project administration. **Songxue Wang:** Supervision, Resources, Validation, Project administration.

Declaration of Competing Interest

The authors declare that they have no known competing financial interests or personal relationships that could have appeared to influence the work reported in this paper.

References

- Chen, T., Li, Y., Meng, S., Liu, C., Liu, D., Dong, D., & You, T. (2022). Temperature and pH tolerance ratiometric aptasensor: Efficiently self-calibrating electrochemical detection of aflatoxin B1. *Talanta*, 242, Article 123280. <https://doi.org/10.1016/j.talanta.2022.123280>
- Commission, E. (2006). Setting of maximum levels for certain contaminants in foodstuffs. *Regulation*, 1881, 5–24.
- Ellington, A. D., & Szostak, J. W. (1990). In vitro selection of RNA molecules that bind specific ligands. *Nature*, 346(6287), 818–822. <https://doi.org/10.1038/346818a0>
- Er Demirhan, B., & Demirhan, B. (2022). Investigation of Twelve Significant Mycotoxin Contamination in Nut-Based Products by the LC-MS/MS Method. *Metabolites*, 12(2), 120. <https://doi.org/10.3390/metabo12020120>
- Fan, T., Xie, Y., & Ma, W. (2021). Research progress on the protection and detoxification of phytochemicals against aflatoxin B1-induced liver toxicity. *Toxicol*, 195, 58–68. <https://doi.org/10.1016/j.toxicol.2021.03.007>
- He, H., Sun, D.-W., Pu, H., & Huang, L. (2020). Bridging Fe3O4@ Au nanoflowers and Au@ Ag nanospheres with aptamer for ultrasensitive SERS detection of aflatoxin B1. *Food Chemistry*, 324, Article 126832. <https://doi.org/10.1016/j.foodchem.2020.126832>
- Hosseini, M., Khabbaz, H., Dadmehr, M., Ganjali, M. R., & Mohamadnejad, J. (2015). Aptamer-based colorimetric and chemiluminescence detection of aflatoxin B1 in foods samples. *Acta Chimica Slovenica*, 62(3), 721–728. <https://doi.org/10.17344/acs.2015.1358>
- Huang, Y., Ma, Y., Chen, Y., Wu, X., Fang, L., Zhu, Z., & Yang, C. J. (2014). Target-responsive DNzyme cross-linked hydrogel for visual quantitative detection of lead. *Analytical chemistry*, 86(22), 11434–11439. <https://doi.org/10.1021/ac503540q>
- Jahangiri-Dehaghani, F., Zare, H. R., Shekari, Z., & Benvidi, A. (2022). Development of an electrochemical aptasensor based on Au nanoparticles decorated on metal-organic framework nanosheets and p-biphenol electroactive label for the measurement of aflatoxin B1 in a rice flour sample. *Analytical and Bioanalytical Chemistry*, 1–13. <https://doi.org/10.1007/s00216-021-03833-3>

- Lerdri, J., Thunkhamrak, C., & Jakkumee, J. (2021). Development of a colorimetric aptasensor for aflatoxin B1 detection based on silver nanoparticle aggregation induced by positively charged perylene diimide. *Food Control*, 130, Article 108323. <https://doi.org/10.1016/j.foodcont.2021.108323>
- Li, M., Wang, H., Sun, J., Ji, J., Ye, Y., Lu, X., ... Sun, X. (2021). Rapid, on-site, and sensitive detection of aflatoxin M1 in milk products by using time-resolved fluorescence microsphere test strip. *Food Control*, 121, Article 107616. <https://doi.org/10.1016/j.foodcont.2020.107616>
- Liu, H., Zhao, Y., Lu, A., Ye, J., Wang, J., Wang, S., & Luan, Y. (2020). An aptamer affinity column for purification and enrichment of aflatoxin B1 and aflatoxin B2 in agro-products. *Analytical and Bioanalytical Chemistry*, 412(4), 895–904. <https://doi.org/10.1007/s00216-019-02300-4>
- Liu, R., Huang, Y., Ma, Y., Jia, S., Gao, M., Li, J., ... Chen, Y. (2015). Design and synthesis of target-responsive aptamer-cross-linked hydrogel for visual quantitative detection of ochratoxin A. *ACS Applied Materials & Interfaces*, 7(12), 6982–6990. <https://doi.org/10.1021/acsami.5b01120>
- Ma, Y., Mao, Y., An, Y., Tian, T., Zhang, H., Yan, J., ... Yang, C. J. (2018). Target-responsive DNA hydrogel for non-enzymatic and visual detection of glucose. *Analyst*, 143(7), 1679–1684. <https://doi.org/10.1039/C8AN00010G>
- Ma, Y., Mao, Y., Huang, D., He, Z., Yan, J., Tian, T., ... Zhu, Z. (2016). Portable visual quantitative detection of aflatoxin B1 using a target-responsive hydrogel and a distance-readout microfluidic chip. *Lab on a Chip*, 16(16), 3097–3104. <https://doi.org/10.1039/C6LC00474A>
- Mao, Y., Li, J., Yan, J., Ma, Y., Song, Y., Tian, T., ... Yang, C. (2017). A portable visual detection method based on a target-responsive DNA hydrogel and color change of gold nanorods. *Chemical Communications*, 53(47), 6375–6378. <https://doi.org/10.1039/C7CC01360D>
- Ni, S., Zhuo, Z., Pan, Y., Yu, Y., Li, F., Liu, J., ... Wan, Y. (2020). Recent progress in aptamer discoveries and modifications for therapeutic applications. *ACS Applied Materials & Interfaces*, 13(8), 9500–9519. <https://doi.org/10.1021/acsami.0c05750>
- Qi, X., Lv, L., Wei, D., Lee, J. J., Niu, M., Cui, C., & Guo, Z. (2022). Detection of aflatoxin B1 with a new label-free fluorescence aptasensor based on PVP-coated single-walled carbon nanohorns and SYBR Gold. *Analytical and Bioanalytical Chemistry*, 1–8. <https://doi.org/10.1007/s00216-022-03938-3>
- Sarwat, A., Rauf, W., Majeed, S., De Boevre, M., De Saeger, S., & Iqbal, M. (2022). LC-MS/MS based appraisal of multi-mycotoxin co-occurrence in poultry feeds from different regions of Punjab, Pakistan. *Food Additives & Contaminants: Part B*, 1–17. <https://doi.org/10.1080/19393210.2022.2037722>
- Setlem, S. K., Mondal, B., & Ramlal, S. (2022). A fluorescent aptasensor for the detection of Aflatoxin B1 by graphene oxide mediated quenching and release of fluorescence. *Journal of Microbiological Methods*, 106414. <https://doi.org/10.1016/j.mimet.2022.106414>
- Si, Y., Li, L., Wang, N., Zheng, J., Yang, R., & Li, J. (2019). Oligonucleotide cross-linked hydrogel for recognition and quantitation of microRNAs based on a portable glucometer readout. *ACS Applied Materials & Interfaces*, 11(8), 7792–7799. <https://doi.org/10.1021/acsami.8b21727>
- Sun, Y., Li, S., Chen, R., Wu, P., & Liang, J. (2020). Ultrasensitive and rapid detection of T-2 toxin using a target-responsive DNA hydrogel. *Sensors and Actuators B: Chemical*, 311, Article 127912. <https://doi.org/10.1016/j.snb.2020.127912>
- Tang, L., Huang, Y., Lin, C., Qiu, B., Guo, L., Luo, F., & Lin, Z. (2020). Highly sensitive and selective aflatoxin B1 biosensor based on Exonuclease I-catalyzed target recycling amplification and targeted response aptamer-crosslinked hydrogel using electronic balances as a readout. *Talanta*, 214, Article 120862. <https://doi.org/10.1016/j.talanta.2020.120862>
- Tian, T., Wei, X., Jia, S., Zhang, R., Li, J., Zhu, Z., ... Yang, C. J. (2016). Integration of target responsive hydrogel with cascaded enzymatic reactions and microfluidic paper-based analytic devices (μPADs) for point-of-care testing (POCT). *Biosensors and Bioelectronics*, 77, 537–542. <https://doi.org/10.1016/j.bios.2015.09.049>
- Wang, B., Chen, Y., Wu, Y., Weng, B., Liu, Y., Lu, Z., ... Yu, C. (2016). Aptamer induced assembly of fluorescent nitrogen-doped carbon dots on gold nanoparticles for sensitive detection of AFB1. *Biosensors and Bioelectronics*, 78, 23–30. <https://doi.org/10.1016/j.bios.2015.11.015>
- Wang, C., Zhang, L., Luo, J., Qin, J., Jiang, J., Qin, L., ... Yang, M. (2021). Development of a sensitive indirect competitive enzyme-linked immunosorbent assay for high-throughput detection and risk assessment of aflatoxin B1 in animal-derived medicines. *Toxicol*, 197, 99–105. <https://doi.org/10.1016/j.toxicol.2021.04.009>
- Wei, X., Tian, T., Jia, S., Zhu, Z., Ma, Y., Sun, J., ... Yang, C. J. (2016). Microfluidic distance readout sweet hydrogel integrated paper-based analytical device (μDISH-PAD) for visual quantitative point-of-care testing. *Analytical chemistry*, 88(4), 2345–2352. <https://doi.org/10.1021/acs.analchem.5b04294>
- Wu, J., Zhu, Y., Xue, F., Mei, Z., Yao, L., Wang, X., ... Peng, C. (2014). Recent trends in SELEX technique and its application to food safety monitoring. *Microchimica Acta*, 181(5), 479–491. <https://doi.org/10.1007/s00604-013-1156-7>
- Wu, Y., Ye, J., Xuan, Z., Li, L., Wang, H., Wang, S., ... Wang, S. (2021). Development and validation of a rapid and efficient method for simultaneous determination of mycotoxins in coix seed using one-step extraction and UHPLC-HRMS. *Food Additives & Contaminants: Part A*, 38(1), 148–159. <https://doi.org/10.1080/19440049.2020.1833089>
- Xiang, X., Ye, Q., Shang, Y., Li, F., Zhou, B., Shao, Y., ... Chen, M. (2021). Quantitative detection of aflatoxin B1 using quantum dots-based immunoassay in a recyclable gravity-driven microfluidic chip. *Biosensors and Bioelectronics*, 190, Article 113394. <https://doi.org/10.1016/j.bios.2021.113394>
- Xie, Y., Wang, W., & Zhang, S. (2019). Purification and identification of an aflatoxin B1 degradation enzyme from *Pantoea* sp. T6. *Toxicol*, 157, 35–42. <https://doi.org/10.1016/j.toxicol.2018.11.290>

- Xuan, Z., Liu, H., Ye, J., Li, L., Tian, W., & Wang, S. (2020). Reliable and disposable quantum dot-based electrochemical immunosensor for aflatoxin B1 simplified analysis with automated magneto-controlled pretreatment system. *Analytical and Bioanalytical Chemistry*, 412(27), 7615–7625. <https://doi.org/10.1007/s00216-020-02897-x>
- Xuan, Z., Ye, J., Zhang, B., Li, L., Wu, Y., & Wang, S. (2019). An automated and high-throughput immunoaffinity magnetic bead-based sample clean-up platform for the determination of aflatoxins in grains and oils using UPLC-FLD. *Toxins*, 11(10), 583. <https://doi.org/10.3390/toxins11100583>
- Yan, T., Zhu, J., Li, Y., He, T., Yang, Y., & Liu, M. (2022). Development of a biotinylated nanobody for sensitive detection of aflatoxin B1 in cereal via ELISA. *Talanta*, 239, Article 123125. <https://doi.org/10.1016/j.talanta.2021.123125>
- Zhang, H., Mao, W., Hu, Y., Wei, X., Huang, L., Fan, S., ... Fu, F. (2022). Visual detection of aflatoxin B1 based on specific aptamer recognition combining with triple amplification strategy. *Spectrochimica Acta Part A: Molecular and Biomolecular Spectroscopy*, 120862. <https://doi.org/10.1016/j.saa.2022.120862>
- Zhong, T., Li, S., Li, X., JiYe, Y., Mo, Y., Chen, L., ... Luo, Q. (2022). A label-free electrochemical aptasensor based on AuNPs-loaded zeolitic imidazolate framework-8 for sensitive determination of aflatoxin B1. *Food Chemistry*, 384, Article 132495. <https://doi.org/10.1016/j.foodchem.2022.132495>